Research

New Phytologist

The Kok effect revisited

Xinyou Yin, Yuxi Niu, Peter E. L. van der Putten and Paul C. Struik

Centre for Crop Systems Analysis, Department of Plant Sciences, Wageningen University & Research, PO Box 430, Wageningen 6700 AK, the Netherlands

Author for correspondence:
Xinyou Yin
Tel: +31 317 482348
Email: Xinyou.Yin@wur.nl

Received: *19 February 2020*
Accepted: *24 April 2020*

New Phytologist (2020) **227:** 1764–1775
doi: 10.1111/nph.16638

Key words: day respiration, Kok method, photorespiration, photosystem II efficiency, reassimilation, Yin method.

Summary

• The Kok effect refers to the abrupt decrease around the light compensation point in the slope of net photosynthetic rate vs irradiance. Arguably, this switch arises from light inhibition of respiration, allowing the Kok method to estimate day respiration (R_d). Recent analysis suggests that increasing proportions of photorespiration (quantified as Γ^*/C_c, the ratio of CO_2 compensation point Γ^* to chloroplast CO_2 concentration, C_c) with irradiance explain much of the Kok effect. Also, the Kok method has been modified to account for the decrease in PSII photochemical efficiency (Φ_2) with irradiance.

• Using a model that illustrates how varying R_d, Γ^*/C_c, Φ_2 and proportions of alternative electron transport could engender the Kok effect, we quantified the contribution of these parameters to the Kok effect measured in sunflower across various O_2 and CO_2 concentrations and various temperatures.

• Overall, the decreasing Φ_2 with irradiance explained *c.* 12%, and the varying Γ^*/C_c explained *c.* 25%, of the Kok effect. Maximum real light inhibition of R_d was much lower than the inhibition derived from the Kok method, but still increased with photorespiration.

• Photorespiration had a dual contribution to the Kok effect, one via the varying Γ^*/C_c and the other via its participation in light inhibition of R_d.

Introduction

The Kok effect refers to the abrupt change in the slope of the linear relationship between net photosynthetic rate and irradiance that occurs at very low irradiances, as observed initially in unicellular algae (Kok, 1948, 1949; Healey & Myers, 1971). The switch is reported later in leaves of many higher plant species (e.g. Ishii & Schmid, 1981; Sharp *et al.*, 1984; Villar *et al.*, 1994; Buckley *et al.*, 2017). The slope decreases from the initial higher value to a lower value, mostly at an irradiance value around the light compensation point. This switch has been interpreted as a consequence of light inhibition of respiration, allowing the so-called Kok method to estimate respiration in the light, or day respiration (R_d), and quantum yield of CO_2 assimilation (Φ_{CO2}) (see Supporting Information Table S1 for all symbol definitions), using the part of the relationship with the lower slope. The absolute value of the estimated R_d is lower than the respiration in the dark (R_{dk}) (Fig. 1). The cost of total respiratory activities accounts for *c.* 40% of gross photosynthetic productivity of whole plants (Gifford, 1995; Amthor, 2010). Light inhibition of respiratory activities also occurs at a stand scale (Gong *et al.*, 2017), suggesting that it is a general phenomenon, and thus would have a significant impact on projecting the net ecosystem carbon fluxes in biomes across the globe (Heskel *et al.*, 2013). For this reason, understanding the Kok effect and its related light inhibition of respiration has continuously received attention (Tcherkez *et al.*, 2017a,b).

The lower estimates of R_d by the Kok method, relative to R_{dk}, have been confirmed by other gas exchange-based methods such as the popular Laisk method (Laisk, 1977). By applying the Laisk method to different light intensities, it has been shown that R_d was progressively inhibited by increasing irradiance (Brooks & Farquhar, 1985; Villar *et al.*, 1995). However, this light inhibition has been challenged by the direct measurement of R_d, which exploits the differences in the time course of labelling by carbon isotopes of photosynthetic, photorespiratory and respiratory pathways. For example, using such techniques, Pinelli & Loreto (2003) suggested a significant refixation of respired and photorespired CO_2 and Loreto *et al.* (2001) calculated that there would be no significant difference between R_d and R_{dk} if the refixation of CO_2 released from respiration during illumination were taken into account. Similarly, a recent report using a direct method based on isotopic disequilibrium (Gong *et al.*, 2018) showed that R_d was underestimated by the Laisk method. Owing to inconsistent reports of this kind, whether the Kok effect was a result of light inhibition of leaf respiration has been under debate over years.

In fact, according to an extended form of the widely used model of Farquhar *et al.* (1980) for describing the electron transport-limited photosynthesis, several other mechanisms could also explain the Kok effect. The extended model expresses the net CO_2 assimilation rate (A) as a function of the photosynthetically absorbed irradiance (I_{abs}) as (Yin *et al.*, 2004, 2006):

$$A = \frac{1 - \Gamma_*/C_c}{4(1 + 2\Gamma_*/C_c)} f_{aet}(\Phi_2 \rho_2 I_{abs}) - R_d \qquad \text{Eqn 1}$$

where C_c is the CO_2 concentration at the carboxylating sites of Rubisco, Γ^* is the CO_2 compensation point in the absence of R_d,

Φ_2 is the photochemical efficiency of photosystem II (PSII) electron transport, ρ_2 is the fraction of the absorbed photons partitioned to PSII, and f_{aet} is the factor accounting for fractions of alternative electron transport. So, the term ($\Phi_2\,\rho_2 I_{abs}$) is the flux of PSII electron transport. Parameters f_{aet} and ρ_2 can be quantified by the extended model as (Yin *et al.*, 2006):

$$f_{aet} = 1 - \frac{f_{pseudo}}{1 - f_{cyc}} \qquad \text{Eqn 2}$$

$$\rho_2 = \frac{1 - f_{cyc}}{1 - f_{cyc} + \frac{\Phi_2}{\Phi_1}} \qquad \text{Eqn 3}$$

where Φ_1 is the photochemical efficiency of PSI electron transport, f_{cyc} is the fraction of the PSI electron flux that follows the cyclic electron transport around PSI, and f_{pseudo} is the fraction of the PSI electron flux that follows the pseudocyclic electron transport (defined as all noncyclic electron-consuming pathways other than the Calvin cycle or the photorespiratory cycle).

Eqn (1) suggests that changes not only in R_d (Fig. 2a), but also in Γ^*/C_c, Φ_2, f_{aet} and ρ_2, with increasing I_{abs}, result in changes in the slope of A vs I_{abs}. Notably, Farquhar & Busch (2017) recently demonstrated that as a result of regulation of stomatal conductance (g_s) and mesophyll conductance (g_m), C_c decreased (thus Γ^*/C_c increased) sharply with increasing I_{abs} within the range of low irradiances, and that this phenomenon accounted for much of the observed Kok effect (Fig. 2b). A similar argument might be applied to Φ_2 (Fig. 2c), as Φ_2 is not constant but decreases with increasing I_{abs} (Genty & Harbinson, 1996), even within the range of low irradiances within which the Kok method is used to estimate R_d and Φ_{CO2} (Yin *et al.*, 2011a, 2014). Accounting for the decrease of Φ_2 with increasing irradiance has resulted in a modified method to estimate R_d (Yin *et al.*, 2009, 2011a). The analysis using the modified method, now known as the Yin method (Tcherkez *et al.*, 2017b), indicates that the inhibition of R_d by light is less than the original Kok method suggests (Yin *et al.*, 2011a).

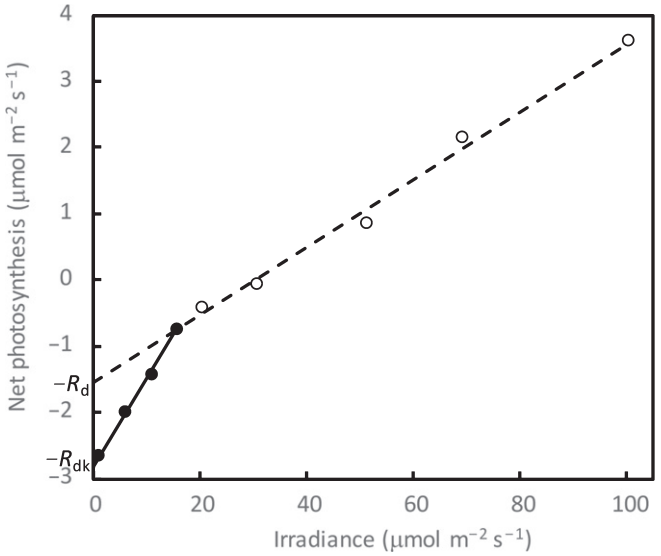

Fig. 1 Illustration of a two-phase photosynthetic response to low irradiances – the Kok effect. The early interpretation of this effect, as suppressing respiration by light, gave rise to the Kok method to estimate respiration in the light (or 'day respiration', R_d, the intercept of phase 2; open symbols with the dashed line), which is lower than respiration in the dark (R_{dk}), the intercept of phase 1 (closed symbols with the solid line).

Less information is available on the change in f_{aet} or in ρ_2 with I_{abs} that could partly explain the Kok effect. Peltier & Sarrey (1988) indicated that the inhibition of chlororespiration (a process in chloroplasts that involves a respiratory electron transport chain within the thylakoid membrane) might be responsible for the Kok effect. Data of Zhang *et al.* (2018) and Ver Sagun *et al.* (2019) suggested that cyclic electron transport around PSI increased with increasing I_{abs}. If this also applies to the limiting light conditions, an increase in f_{cyc} with increasing I_{abs} would predict a part of the Kok effect (Fig. 2d). According to Eqns 2 and 3, f_{cyc} has a dual effect on the expression of the Kok effect, that is, via both terms f_{aet} and ρ_2. Eqn 3 suggests that parameter ρ_2, related to state transition, could be affected not only by f_{cyc} (Fig. 2d) but also by the Φ_2/Φ_1 ratio. Tcherkez *et al.* (2017a) speculated the possible role of state transition in the Kok effect. The model of Eqns 1–3 predicts that an increase in f_{cyc} or in Φ_2/Φ_1 with increasing I_{abs} leads to the state transition in favour of PSI with increasing irradiance, and this could engender part of the Kok effect (Fig. 2d).

The Kok effect is not ubiquitous. Early reports found little Kok effect at low O_2 conditions and in C_4 plants (Cornic & Jarvis, 1978; Ishii & Murata, 1978). These observations have led to suggestions that photorespiration might be involved in the Kok effect, as confirmed by other studies where photorespiration was manipulated by changing measurement temperatures (Ishii & Schmid, 1981; Way *et al.*, 2019) or by lowering leaf water potential (Sharp *et al.*, 1984). Again, the model analyses of Farquhar & Busch (2017) demonstrated that the change in Γ^*/C_c, therefore, in relative amounts of photorespiration, with increasing I_{abs} can explain much of the diminution of the Kok effect in C_4 plants and at low O_2 or high CO_2 concentrations or low temperatures. They also showed that the change in Γ^*/C_c can generate the apparent inhibition of R_d as inferred by the Laisk method, which is based on A–C_i curves at two or more irradiances (where C_i is the intercellular CO_2 concentration). The decrease in C_i with increasing I_{abs} is the result of stomatal regulation, and its influence on estimates of R_d by the Kok method was noted by Kirschbaum & Farquhar (1987), who proposed a method to correct for this decrease in C_i. The further drawdown in C_c, relative to C_i, is regulated by g_m (Evans & von Caemmerer, 1996). The Kok method would underestimate R_d if light-dependent changes in C_i (Villar *et al.*, 1994) or in C_c (Ayub *et al.*, 2011) are not corrected for. Simple g_s and g_m models when coupled with photosynthesis models like Eqns 1–3 can account for the refixation of CO_2 released from respiration and photorespiration (von Caemmerer, 2013), and in fact, the refixation fractions of (photo) respired CO_2 can be calculated analytically from stomatal, mesophyll and carboxylation resistances (Yin & Struik, 2017). As such, the light inhibition of R_d predicted for photorespiratory conditions by Farquhar & Busch (2017) and the need to correct

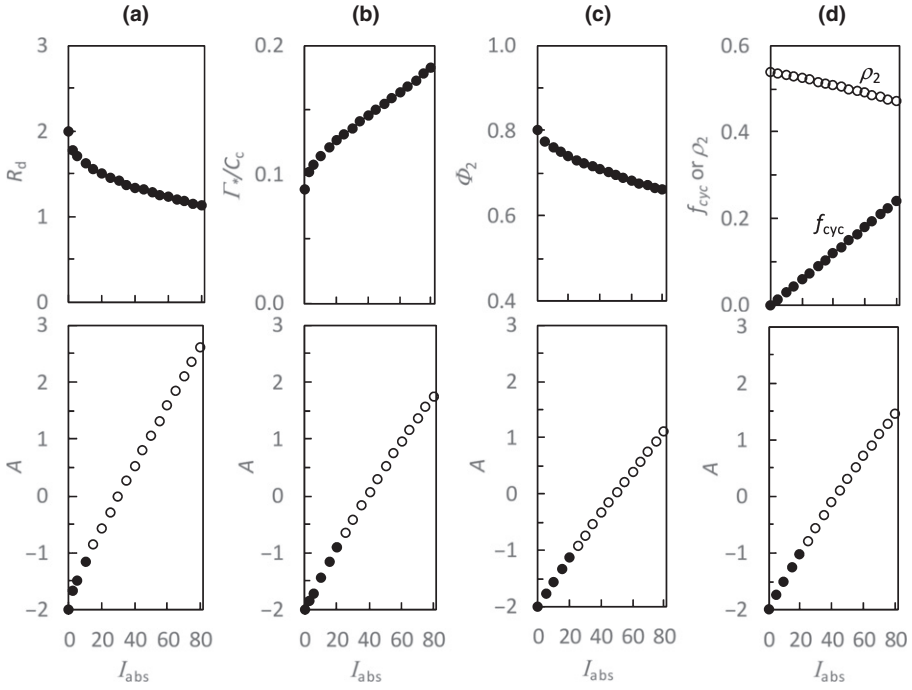

Fig. 2 Illustration of the impact of varying values of four parameters (day respiration, R_d; ratio of CO_2 compensation point to chloroplast CO_2 concentration, Γ^*/C_c; photosystem II photochemical efficiency, Φ_2; and fraction for cyclic electron transport, f_{cyc}) with absorbed irradiance I_{abs} (upper panels of a–d, respectively) on the shape of the light response curve of net photosynthesis (A, lower panels), where there seems to be a transition from a higher-slope phase (closed symbols) to a lower-slope phase (open symbols). Curves in lower panels are generated from Eqns 1–3, in which, when showing the impact of one parameter, other parameters were kept constant. Units are as follows: I_{abs}, μmol m^{-2} s^{-1}; R_d and A, μmol m^{-2} s^{-1}; Φ_2, mol mol^{-1}; Γ^*/C_c, unitless; and f_{cyc} and excitation partitioning to PSII ρ_2, fractions.

for light-dependent changes in C_i and C_c are basically analogous to the statement of Loreto *et al.* (2001) that the lower R_d than R_{dk} resulted from the failure of the original Kok or Laisk methods in accounting for the refixation of respired CO_2 in the light.

However, there are cases where the Kok effect is not always associated with photorespiration. The change in the slope was occasionally observed to be present under high-CO_2 conditions (Sharp *et al.*, 1984), and in C_4 leaves and under low-O_2 conditions albeit to a smaller extent (Yin *et al.*, 2011a). Gong *et al.* (2015) reported an even lower $R_d : R_{dk}$ ratio in C_4 than in C_3 leaves. Buckley *et al.* (2017) observed a similar extent of change in the slope under both 21% and 2% O_2 conditions for broadbean (*Vicia faba*) mature leaves. Nevertheless, the Kok effects reported in the early years (Kok, 1949; Ishii & Schmid, 1981; Sharp *et al.*, 1984) are mostly associated with the abrupt transition in the slope (Fig. 1), whereas the g_s–g_m photosynthesis model predicts only a smooth transition (Farquhar & Busch, 2017).

Of the possible mechanisms (R_d, Γ^*/C_c, Φ_2, f_{aet} and/or ρ_2) highlighted by Eqns 1–3 that potentially explain the magnitude of the Kok effect (Fig. 2), f_{aet} and ρ_2 are hard to measure accurately by existing equipment, especially at low irradiances along the Kok curve. Also, the pattern of changing R_d in response to I_{abs} is hard to quantify with existing methods. In this study, we will illustrate, using Eqns 1–3, that how R_d responds to I_{abs} would have relevance to the Kok effect and in estimating Φ_{CO2}. We surmise that if the varying Γ^*/C_c ratio is a major factor accounting for the Kok effect, as stated by Farquhar & Busch (2017), then the magnitude of the Kok effect should be associated with the Γ^*/C_c ratio, regardless of how the variation of this ratio is created. To this end, we designed an experiment in which we used various O_2 and CO_2 concentrations or temperatures to generate varying relative amounts of photorespiration, that is, various Γ^*/C_c ratios. Based on a modelling analysis of the experimental data we quantitatively assess: whether the change of Γ^*/C_c and the decrease of Φ_2 with increasing I_{abs} could explain, in part, the Kok effect; if so, what the relative contribution of the two components is in determining the Kok effect; and what the maximum real inhibition of R_d by light is. We demonstrate that our results help to identify common threads explaining seemingly contradictory findings among previous studies on R_d.

Materials and Methods

Plant materials and measurements

Plants of sunflower (*Helianthus annuus*, cv 'Sunspot') were grown in pots in a growth chamber (day : night temperature, 25 : 20°C; relative humidity, 70%; photon flux density, *c.* 500 μmol m^{-2} s^{-1} at the soil level; photoperiod, 16 h, 06:00–22:00 h) in Wageningen. Five seeds were sown and seedlings were thinned to one plant per 7 l pot. Initial amounts of soil nitrogen (N), phosphorus (P) and potassium (K) were 0.62, 0.83, and 1.04 g per pot, respectively. Nutrient solution was added two or three times per week based on the expected plant growth. Seeds were sown weekly for 4 wk, creating four replications. Measurements were conducted on the 11th or 12th fully expanded leaf counting from the bottom, using one plant per replication.

An open gas exchange system (Li-Cor 6800; Li-Cor Inc., Lincoln, NE, USA) and an integrated fluorescence chamber head of 6 cm^2 were used for three sets of measurements, in which various O_2 or CO_2 concentrations or various temperatures were used to create different amounts of photorespiration (Table 1). The first set used five O_2 concentrations. Four cylinders containing different mixtures of O_2 and N_2 were used. Gas from the cylinder was supplied to the Li-Cor 6800 where CO_2 was blended with O_2. For the second set, five different ambient CO_2 (C_a)

concentrations in the leaf chamber were used (Table 1). For the third set, four leaf temperatures were used (Table 1). A flow rate of 200 μmol s^{-1} was used, and leaf-to-air vapour pressure difference was maintained within 0.8–1.6 kPa, for all measurements.

For a given O_2, CO_2 or temperature, a photosynthetic response curve to incident irradiance ($A-I_{inc}$) was measured. Leaves were first acclimated under 80 μmol m^{-2} s^{-1} until A reached a steady state, which took *c.* 45 min. Measurements were then undertaken using a sequence of 80, 70, 60, 50, 40, 30, 25, 20, 15, 10, and 5 μmol m^{-2} s^{-1}, with 6 min for each step. For measurements in each of the first two sets, O_2 or CO_2 concentrations were chosen randomly. Measurements of the temperature set were conducted after the O_2 and CO_2 sets to avoid possible after-effects of high temperature on leaves. For the same reason, the four temperatures were set up from low to high rather than randomly.

After the measurements for $A-I_{inc}$ curves, $A-C_i$ curves were determined to provide extra data to estimate g_m. Leaves were adapted to an I_{inc} of 100 μmol m^{-2} s^{-1} at 25°C and 21% O_2 until A became stable, and curves were measured using a C_a sequence of 400, 200, 100, 75, 50, 400, 400, 550, 800 and 1500 μmol mol^{-1}, with 3 min per step. Apparent A–C_i curves were also assessed with heat-killed leaves, which showed that CO_2 leakage was negligible during our measurement using the Li-Cor 6800.

For each step of either the $A-I_{inc}$ or $A-C_i$ curve, PSII photochemical operating efficiency (Φ_2) was determined by Chl fluorescence as $(1-F_s/F_m')$, where F_s is the steady-state fluorescence and F_m' is the maximum fluorescence as revealed using the single flash of *c.* 8500 μmol m^{-2} s^{-1} for a duration of 1.0 s. We did not use the multiphase method to determine F_m' because all measurements were undertaken at low irradiances.

Leaf spots used for measurements were punched out, and leaf discs were measured for light absorption (STS-VIS miniature spectrometer; Ocean Optics, Dunedin, FL, USA), twice per disc, to represent average absorption at this spot. After measuring their areas, leaf discs were dried in a 70°C oven for 24 h to determine dry matter. Each dry leaf disc was then ground into powder, and samples of 1–3 mg were analysed for N concentrations with an EA1108 CHN-O Element Analyzer (Fisons Instruments, Waltham, MA, USA) using the Dumas combustion method.

Data and modelling analyses

All the leaf spots had a similar N content. The average leaf N was 1.6 g m^{-2} and average leaf absorptance was 85%. Variation among replications was small, and replicate average values were used for analysis.

Table 1 Levels of O_2, ambient CO_2 and leaf temperature in three sets of measurements on sunflower leaves.

Set	O_2 (%)	CO_2 (μmol mol^{-1})	Temperature (°C)
1	2, 10, 21, 35, 50	400	25
2	21	100, 250, 400, 550, 700	25
3	21	400	15, 25, 30, 35

Data of A vs I_{abs} were inspected to identify the irradiance at the Kok transition point ($I_{abs,t}$), based on the highest average r^2 of linear regression on points both below and above the candidate $I_{abs,t}$ of each curve. The regression slopes below and above $I_{abs,t}$ were denoted as b_1 and b_2, respectively, and the $b_1 : b_2$ ratio was calculated. The intercept of the regression after $I_{abs,t}$ is the day respiration estimated by the Kok method. Here, the intercepts of regression lines before and after $I_{abs,t}$ are denoted as r_{d1} and r_{d2}, respectively. According to the original interpretation of the Kok effect (Fig. 1), r_{d1} is equivalent to the respiration rate in the darkness, R_{dk}.

To examine if the decrease of Φ_2 with increasing I_{abs} could partly explain the Kok effect, plots of A vs I_{abs} Φ_2 were made. To be compared with the $A-I_{abs}$ plots, data points were allocated according to $I_{abs,t}$ identified earlier, and linear regression slopes both below and above $I_{abs,t}$ were denoted as B_1 and B_2, respectively. Any decrease in the $B_1 : B_2$ ratio, relative to the $b_1 : b_2$ ratio, would suggest that the decrease of Φ_2 with increasing I_{abs} could partly explain the Kok effect. The intercept of the linear plot of A vs I_{abs} $\Phi_2/4$ after the Kok break point is the day respiration estimated by the Yin method (Yin *et al.*, 2009, 2011a). As the intercept remains unchanged if the linear plot is made here for A vs I_{abs} Φ_2, the intercepts of $A-I_{abs}$ Φ_2 lines before and after $I_{abs,t}$ are denoted as R_{D1} and R_{D2}, respectively.

To assess the impact of Γ^*/C_c on the Kok effect, C_c has to be known. To that end, we estimated g_m using all data from combined gas exchange and Chl fluorescence measurements. g_m is known to vary with temperature (Bernacchi *et al.*, 2002), but whether g_m varies with C_i or with I_{inc} or O_2 is uncertain. Furthermore, recent literature suggests the necessity to dissect mesophyll resistance into its components (Tholen *et al.*, 2012) and to consider the intracellular arrangements of organelles (Yin & Struik, 2017; Ubierna *et al.*, 2019; Yin *et al.*, 2020). Here we consider three g_m modes: mode i assumes that g_m varies only with temperature, but not with either C_i or I_{inc} or O_2; mode ii assumes that g_m varies with all these factors; and mode iii is similar to mode ii but uses an additional factor m that lumps subresistance proportions and several intracellular properties of mesophyll organelles (Yin *et al.*, 2020). For mode i, we estimated g_m by fitting, the NRH-A method based on the non-rectangular hyperbolic equation for CO_2-assimilation, described by Yin & Struik (2009) to all data (including $A-C_i$ curves). Like photosynthetic rate, g_m has generally an optimum response to temperature (e.g. Bernacchi *et al.*, 2002; Warren & Dreyer, 2006; but with caution, see von Caemmerer & Evans, 2015), and we assumed that this response followed a normal distribution function, with an optimum temperature of 30°C: $g_m = g_{m30} \exp\{-[(T-30)/\Omega]^2\}$, which has a minimum number of parameters to estimate. We incorporated these relationships into the NRH-A method to fit parameter Ω. For modes ii and iii, we used an equation described by Yin *et al.* (2009), $g_m = \delta(A + R_d)/(C_c - \Gamma^*)$, which can semi-empirically accommodate the response (if observed) of g_m to I_{inc}, C_i, O_2 and temperature. Here, it is the unitless coefficient δ that is an explicit parameter to be estimated, and δ represents the carboxylation resistance : mesophyll resistance ratio (Yin *et al.*, 2020). For each mode, the simultaneously estimated parameters together with g_m or δ were: the calibration factor(s) that converts Chl fluorescence-

based PSII photochemical efficiency (Φ_2) into linear electron transport rate (J), with $J = sI_{inc}\,\Phi_2$ (Yin *et al.*, 2009); and Rubisco specificity at 25°C ($S_{c/o25}$). The values of $S_{c/o}$ for other temperatures were calculated from the relation $\Gamma^* = 0.5\,O/S_{c/o}$ (where O is the concentration of oxygen; Farquhar *et al.*, 1980; von Caemmerer, 2013) and the Arrhenius equation using 24 460 J mol^{-1} of Bernacchi *et al.* (2002) as the activation energy for Γ^* (using other activation-energy estimates (e.g. Walker *et al.*, 2013; Yin *et al.*, 2014) had little impact on our calculated Γ^*/C_c ratios). In view of the reasoning of Farquhar & Busch (2017), we used R_{D1} of each curve as input for the R_d term of the model in fitting. The fitting procedures for three modes were implemented using the GAUSS method in PROC NLIN of SAS (SAS Institute Inc, Cary, NC, USA), and the SAS codes can be obtained upon request. The SAS output gave the fitted A for each measurement point, with which C_c was then solved from the model of Farquhar et al. (1980) as: $C_c = \Gamma^*\,[J/4 + 2(A + R_d)]/[J/4 - (A + R_d)]$.

Results

Forms of light inhibition of R_d in relation to the Kok effect

We consider all possible scenarios in interpreting the often-said 'progressive' inhibition of respiration by light, and examine, based on Eqn 1, the consequence of these scenarios on the shape of $A-I_{abs}$ curves within a range of the low irradiances (Fig. 3).

The scenario 'continuously linear decrease' of R_d with light (Fig. 3a) did not at all result in a break in the linear relationship. Only two 'bilinear' scenarios can generate the Kok effect with an abrupt transition point (Fig. 3b,c). The 'continuously decelerating decrease' scenario also generated the Kok effect but without the abrupt break point (Fig. 3d). For an 'accelerating decrease' scenario, R_d was also progressively suppressed by light, but this scenario generated an $A-I_{abs}$ curve where the slope did not decrease but increased (Fig. 3e), thereby being unable to reproduce the Kok curve. Finally, an 'abrupt suppression' scenario cannot be ruled out, but this scenario generated two linear discontinued segments with the same slope (Fig. 3f), thereby being unable to reproduce the Kok effect either.

As illustrated in Fig. 3, the difference in scenarios also has implications for the estimation of Φ_{CO2}. Only in the second 'bilinear' scenario (Fig. 3c) and the abrupt-suppression scenario (Fig. 3f) can Φ_{CO2} be reliably estimated by the Kok method as the slope of the $A-I_{abs}$ curve above the break point. For other scenarios, the slope represents the combined yield of photosynthesis and of the component of light suppression of R_d. In fact, it is the scenario of Fig. 3(c) that the Kok method relies on to estimate R_d and Φ_{CO2}.

The observed Kok effect across various O_2 and CO_2 concentrations and various temperatures

Linear plots of A vs I_{abs} using our experimental data identified the Kok break point in each curve (Fig. 4). The maximum values of the slope below (phase 1, b_1) and above the break point (phase 2, b_2) were achieved at 2% O_2, and were 0.095 and 0.090 mol mol^{-1}, respectively (Table 2), similar to experimentally measured (Long *et al.*, 1993) or theoretically inferred Φ_{CO2} (Yin *et al.*, 2006) for C_3 species under nonphotorespiratory conditions. A change in the slope from phase 1 to phase 2 became more significant with

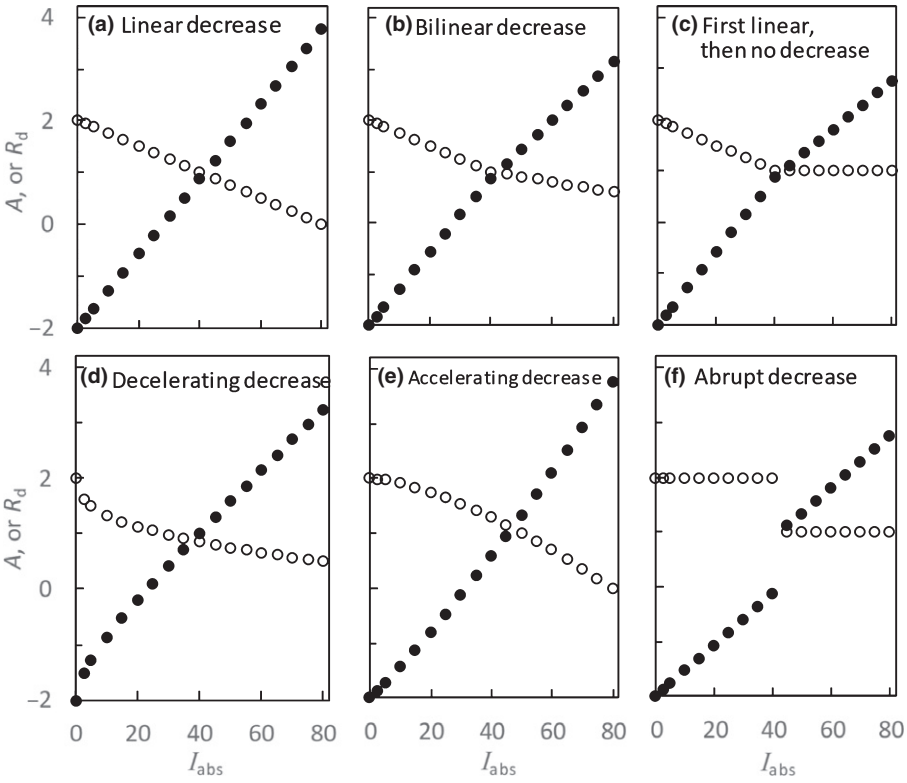

Fig. 3 Illustration of six scenarios (a–f) for the so-called 'progressive' decrease of day respiration, R_d, with absorbed irradiance, I_{abs} (open circles), and their impact on the shape of the light response curve of net photosynthesis, A (closed circles). Units: I_{abs}, μmol m^{-2} s^{-1}; R_d and A, μmol m^{-2} s^{-1}.

increasing O_2 concentrations, with decreasing CO_2 concentrations, and with increasing temperature (Fig. 4). The $b_1 : b_2$ ratio increased from 1.06 at 2% O_2 to 1.69 at 50% O_2, from 1.07 at 700 μmol mol^{-1} CO_2 to 1.83 at 100 μmol mol^{-1} CO_2, and from 1.10 at 15°C to > 1.30 at 30–35°C (Table 2).

Similarly, the difference in the estimated respiration for phase 1 and phase 2, denoted as r_{d1} and r_{d2}, respectively, became more significant with increasing O_2 concentrations, decreasing CO_2 concentrations, and increasing temperature (Table 3). With the estimated b_1, b_2, r_{d1} and r_{d2}, the irradiance for the Kok break point, $I_{abs,t}$, can be calculated, and it varied from 7 to 27 μmol m^{-2} s^{-1} (Table 3).

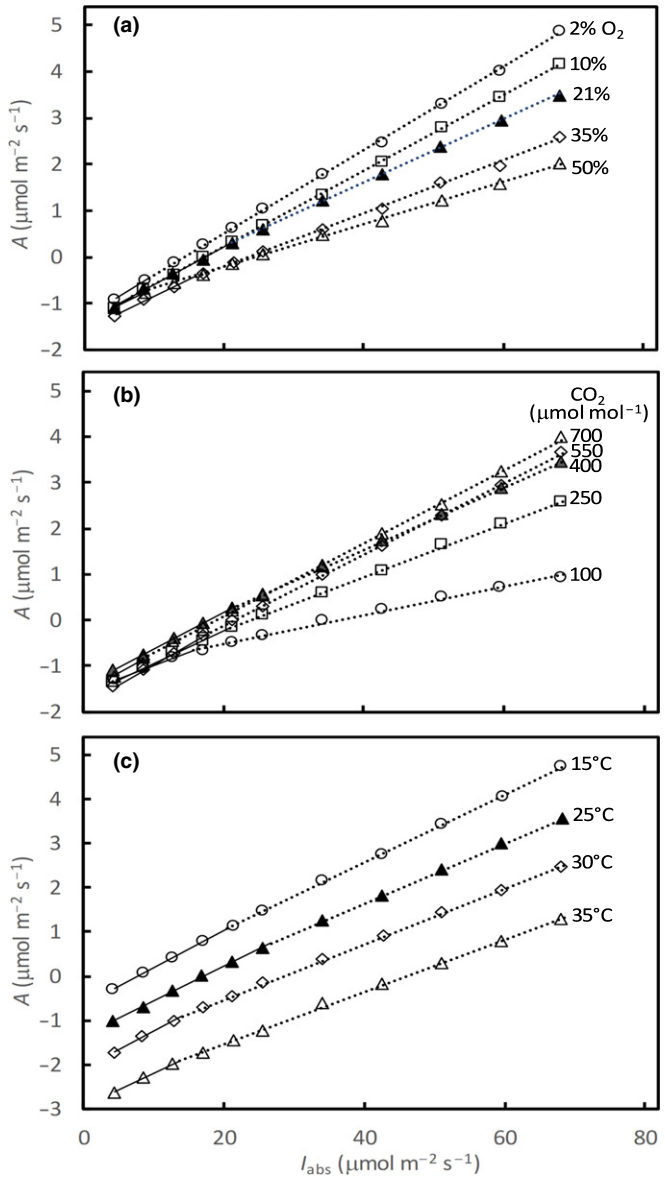

Fig. 4 Net photosynthesis rates (A) vs absorbed irradiance (I_{abs}), based on measured data from five O_2 concentrations (a), five CO_2 concentrations (b), and four temperatures (c) for sunflower leaves. Points represent the means of measurements on four replicated leaves. Continuous lines are for phase 1, and dotted lines are for phase 2, of the Kok plot, drawn from parameter estimates as given in Tables 2 and 3.

The variable Φ_2 as a possible cause for the Kok effect

As with previous reports (Yin *et al.*, 2011a, 2014), Φ_2 decreased with increasing irradiances in all three sets of measurements (Fig. S1). Compared with the A vs I_{abs} plots, the A vs I_{abs} Φ_2 plots had a similar shape (thus, they are not shown), but the obtained $B_1 : B_2$ ratios were slightly lower than the $b_1 : b_2$ ratios (Table 2). As expected, the regression of A against I_{abs} Φ_2 yielded consistently lower intercepts, and therefore higher estimates, R_{D1} and R_{D2}, compared with r_{d1} and r_{d2}, respectively, confirming the results of earlier studies (Yin *et al.*, 2011a). For the same reason, the $R_{D1} : R_{D2}$ ratios were smaller than the $r_{d1} : r_{d2}$ ratios (Table 3). There were no consistent trends for absolute values of r_{d1}, r_{d2}, R_{D1} and R_{D2} with changing O_2 or CO_2 concentrations; but unsurprisingly they increased consistently with increasing temperature (Table 3).

Association of the Kok effect with the variable Γ^*/C_c

We estimated parameter values of the aforementioned three g_m modes. The estimate of the m factor for mode iii was 0, which means that modes ii and iii had identical results. To test whether a nonzero m factor influenced the calculated C_c, we fixed m to 0.3, our recent estimate of this parameter (Yin *et al.*, 2020). The three g_m modes yielded the same goodness of fit with R^2 of 0.966 (Table S2). The modelled A by the three modes did not differ essentially (Fig. S2a). Using the modelled A, we calculated the Γ^*/C_c ratio across irradiance of all the three sets of measurements. The Γ^*/C_c ratios calculated by mode ii or iii at first very low irradiances were more variable than those given by mode i (results not shown), but the average Γ^*/C_c ratio along a given $A-I_{inc}$ curve did not differ much between the three modes (Fig. S2b). We also used the variable J method of Harley *et al* (1992) to inspect any variation of g_m and found no evidence that g_m varied with either C_i or with I_{inc} or with O_2. In the following analysis, we show the results based on the estimate using mode i, as they did not differ much from those using mode ii or iii.

The obtained average Γ^*/C_c ratio varied from 0.008 to 0.195 when O_2 varied from 2% to 50%, from 0.322 to 0.049 when CO_2 varied from 100 to 700 μmol mol^{-1}, and from 0.066 to 0.110 when temperature varied from 15 to 35°C. Plotting the $b_1 : b_2$ ratio or the $B_1 : B_2$ ratio against the Γ^*/C_c ratio showed linear relationships, and because these linear relations did not differ significantly among the three sets of measurements, the common regression line was obtained, and the intercept of the line at the zero Γ^*/C_c ratio was close to 1 (Fig. 5a).

The extents to which the Kok effect was explained by variable Φ_2 and Γ^*/C_c

The strong correlation of the $b_1 : b_2$ or $B_1 : B_2$ ratio with the Γ^*/C_c ratio (with $R^2 > 0.80$; Fig. 5a) does not mean that the varying Γ^*/C_c ratio can explain more than 80% of the Kok effect because other factors (such as R_d and f_{aet}) may vary with Γ^*/C_c as well. However, the relative difference in the slope value between the $b_1 : b_2$ vs the Γ^*/C_c plot (2.559, Fig. 5a) and the $B_1 : B_2$ vs the $\Gamma^*/$

Table 2 Estimates of the slope values of phase 1 (b_1) and phase 2 (b_2) in the *A* vs I_{abs} plot or of the slope values of phase 1 (B_1) and phase 2 (B_2) in the *A* vs $I_{abs}\Phi_2$ plot for sunflower leaves.

		A vs I_{abs} plot			*A* vs $I_{abs}\Phi_2$ plot		
		b_1	b_2	$b_1 : b_2$	B_1	B_2	$B_1 : B_2$
O_2 (%)	2	0.095 (0.004)	0.090 (0.001)	1.06	0.118 (0.004)	0.115 (0.001)	1.03
	10	0.083 (0.003)	0.082 (0.001)	1.02	0.109 (0.003)	0.106 (0.001)	1.02
	21	0.081 (0.003)	0.068 (0.001)	1.19	0.103 (0.003)	0.090 (0.001)	1.15
	35	0.071 (0.005)	0.057 (0.001)	1.24	0.092 (0.006)	0.076 (0.001)	1.21
	50	0.078 (0.011)	0.046 (0.001)	1.69	0.105 (0.014)	0.063 (0.001)	1.67
CO_2 (μmol mol^{-1})	100	0.057 (0.008)	0.031 (0.001)	1.83	0.073 (0.005)	0.042 (0.001)	1.74
	250	0.070 (0.003)	0.058 (0.001)	1.21	0.088 (0.002)	0.075 (0.001)	1.17
	400	0.080 (0.001)	0.068 (0.000)	1.18	0.099 (0.001)	0.086 (0.000)	1.15
	550	0.086 (0.003)	0.078 (0.001)	1.11	0.108 (0.003)	0.101 (0.001)	1.07
	700	0.085 (0.003)	0.080 (0.001)	1.07	0.102 (0.003)	0.103 (0.001)	0.99
Temperature (°C)	15	0.085 (0.002)	0.077 (0.000)	1.10	0.105 (0.002)	0.098 (0.000)	1.06
	25	0.079 (0.001)	0.068 (0.001)	1.16	0.099 (0.001)	0.088 (0.001)	1.13
	30	0.086 (0.004)	0.063 (0.001)	1.37	0.112 (0.004)	0.085 (0.001)	1.32
	35	0.078 (0.006)	0.059 (0.001)	1.33	0.105 (0.006)	0.081 (0.001)	1.29

The slope values have a unit of mol mol^{-1} and standard errors of the estimates are given in brackets; data used for estimation were from the three sets of measurements as described in Table 1.
A, net rate of leaf photosynthesis (μmol m^{-2} s^{-1}); I_{abs}, irradiance absorbed by leaf photosynthetic pigments (μmol m^{-2} s^{-1}); Φ_2, photochemical efficiency of photosystem II electron transport (mol mol^{-1}).

Table 3 Estimates of the intercept values of phase 1 (r_{d1}) and phase 2 (r_{d2}) in the *A* vs I_{abs} plot or of the intercept values of phase 1 (R_{D1}) and phase 2 (R_{D2}) in the *A* vs I_{abs} Φ_2 plot for sunflower leaves.

		A vs I_{abs} plot			*A* vs $I_{abs}\Phi_2$ plot			
		r_{d1}	r_{d2}	$r_{d1} : r_{d2}$	R_{D1}	R_{D2}	$R_{D1} : R_{D2}$	$I_{abs,t}$
O_2 (%)	2	1.33 (0.04)	1.28 (0.04)	1.04	1.34 (0.03)	1.34 (0.03)	1.00	9.1
	10	1.42 (0.03)	1.41 (0.03)	1.01	1.46 (0.03)	1.46 (0.03)	1.00	6.8
	21	1.41 (0.03)	1.14 (0.03)	1.24	1.41 (0.03)	1.21 (0.02)	1.17	21.0
	35	1.55 (0.05)	1.33 (0.05)	1.17	1.56 (0.06)	1.38 (0.05)	1.13	16.0
	50	1.43 (0.07)	1.13 (0.02)	1.26	1.44 (0.07)	1.15 (0.02)	1.25	9.3
CO_2 (μmol mol^{-1})	100	1.55 (0.07)	1.14 (0.04)	1.35	1.55 (0.05)	1.17 (0.03)	1.32	15.6
	250	1.64 (0.03)	1.39 (0.03)	1.18	1.64 (0.02)	1.43 (0.02)	1.15	20.9
	400	1.44 (0.01)	1.16 (0.02)	1.24	1.44 (0.01)	1.21 (0.01)	1.19	21.9
	550	1.83 (0.03)	1.68 (0.03)	1.09	1.83 (0.03)	1.73 (0.03)	1.06	17.4
	700	1.57 (0.04)	1.53 (0.04)	1.03	1.54 (0.04)	1.56 (0.04)	0.99	8.5
Temperature (°C)	15	0.66 (0.02)	0.50 (0.02)	1.32	0.67 (0.01)	0.56 (0.01)	1.18	20.4
	25	1.36 (0.02)	1.06 (0.03)	1.28	1.36 (0.01)	1.12 (0.02)	1.22	26.7
	30	2.10 (0.04)	1.78 (0.02)	1.18	2.10 (0.03)	1.82 (0.02)	1.15	14.0
	35	2.98 (0.06)	2.71 (0.03)	1.10	2.98 (0.06)	2.75 (0.03)	1.08	13.6

The intercept values have a unit of μmol m^{-2} s^{-1} and standard errors of the estimates are given in brackets; data used for estimation were from the three sets of measurements as described in Table 1.
A, net rate of leaf photosynthesis (μmol m^{-2} s^{-1}); I_{abs}, irradiance absorbed by leaf photosynthetic pigments (μmol m^{-2} s^{-1}); Φ_2, photochemical efficiency of photosystem II electron transport (mol mol^{-1}); $I_{abs,t}$, the calculated value of I_{abs} (μmol m^{-2} s^{-1}) for the transition from phase 1 to phase 2 from the *A* vs I_{abs} plot.

C_c plot (2.262; Fig. 5a) should quantify the contribution of the decreasing Φ_2 in explaining the Kok effect. This relative difference was $(2.559–2.226)/2.559 \times 100\% = 11.6\%$, suggesting that, overall, the varying Φ_2 explained *c.* 12% of the Kok effect across varying O_2 and CO_2 concentrations and varying temperatures.

We plotted the modelled *A* against I_{abs} to generate slope values of b_1 and b_2, and thereby the modelled $b_1 : b_2$ ratios. The modelled $b_1 : b_2$ ratios did increase with the Γ^*/C_c ratio (Fig. 5b), in line with the statement of Farquhar & Busch (2017) that the changing Γ^*/C_c ratio explains much of the observed Kok effect. Farquhar & Busch (2017) did not estimate quantitatively the extent of the explanation.

The modelled $b_1 : b_2$ ratios were lower than the observed $b_1 : b_2$ ratios shown in Table 2. Our prediction used measured C_i and Φ_2 as input and took the effect of g_m and Γ^* into account, and therefore the effects of varying Φ_2 and Γ^*/C_c were already considered in the modelling. This suggests that the plot of the modelled $b_1 : b_2$ ratios vs the Γ^*/C_c ratios should reflect the combined effect of both varying Φ_2 and varying Γ^*/C_c. The intercept of the plot for the modelled $b_1 : b_2$ ratios vs the Γ^*/C_c ratios was again close to 1; but its slope was 0.944 (Fig. 5b), much lower

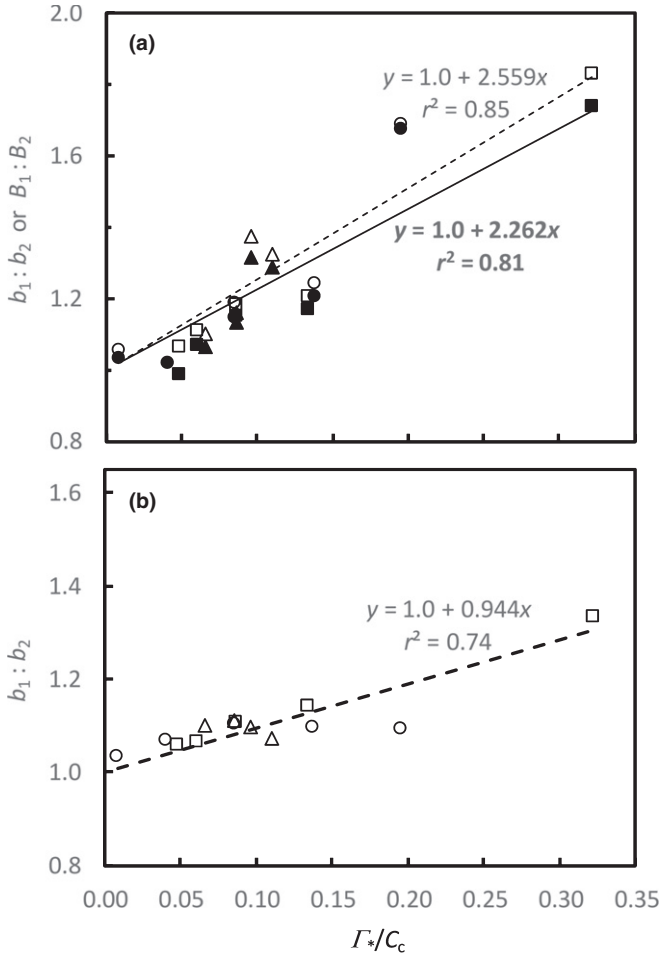

Fig. 5 The slope ratios of phase 1 to phase 2 in the net photosynthesis rate (A) vs absorbed irradiance (I_{abs}) plot (i.e. $b_1 : b_2$ ratios; open symbols) or in the A vs $I_{abs}\Phi_2$ plot (i.e. $B_1 : B_2$ ratios; closed symbols) based on measured values of A (a), or the $b_1 : b_2$ ratios based on modelled values of A (b), plotted against ratios of CO_2 compensation point to chloroplast CO_2 concentration (Γ^*/C_c) across various O_2 concentrations (circles), CO_2 concentrations (squares) and temperatures (triangles) for sunflower leaves. Equations represent the regression lines that pass the (0, 1) point. Φ_2, photosystem II photochemical efficiency.

than 2.559 – the slope of the observed $b_1 : b_2$ ratios vs the Γ^*/C_c ratios (Fig. 5a). As the intercept remained unaltered, this indicates that the combined contribution of varying Φ_2 and Γ^*/C_c to the observed Kok effect can be estimated from slope values, that is, *c.* 36.9% (= 0.944/2.559 × 100%). Therefore, the effect of varying Γ^*/C_c alone explained *c.* 25.3% (36.9–11.6%) of the observed Kok effect across various O_2 and CO_2 concentrations and various temperatures.

Quantifying the maximum extent of inhibition of day respiration by light

Our modelling procedure aimed to quantify the contribution of Φ_2 and varying Γ^*/C_c, and therefore, as is the usual case, assumed that R_d and f_{aet} did not vary with irradiance or with measurement O_2 and CO_2 conditions. The remaining unexplained contributions (*c.* 63%) must be a result of light inhibition of R_d and possibly variable f_{aet} and/or ρ_2. We are not able to separate the contribution of light inhibition of R_d from the effect of variable f_{aet} and/or ρ_2 if the variation of f_{aet} and/or ρ_2 with irradiance cannot be ruled out. If we assume that the variation of either f_{aet} and/or ρ_2 with irradiance is negligible with the limiting light range, as is often assumed in measuring Φ_{CO2}, we can quantify the real inhibition of R_d by light by removing the effect of changing Φ_2 and Γ^*/C_c, as described in the following. As such, this estimate should be considered as the maximum real inhibition of R_d by light.

The apparent relative inhibition in case of the Yin method is:

$$\text{Inhibition}_{\text{apparent}}(\%) = \frac{R_{\text{D1measured}} - R_{\text{D2measured}}}{R_{\text{D1measured}}} \times 100 \quad \text{Eqn 4}$$

The similar apparent relative inhibition can be proposed for the Kok method. The apparent inhibition was higher according to the Kok method than according to the Yin method (Fig. 6a), owing to the fact that the Kok method ignores the decrease of Φ_2 with irradiance. Overall, the Kok method overestimated the apparent inhibition of R_d by *c.* 18%, as compared with the Yin method.

Plotting the modelled A against I_{abs} resulted in lower estimates of r_{d2} than r_{d1} and plotting the modelled A against I_{abs} Φ_2 also resulted in lower estimates of R_{D2} than R_{D1} than their respective estimates using the observed A (results not shown), although a single value of R_d was used for each curve in modelling. This confirmed the analysis of Farquhar & Busch (2017) that the apparent inhibition of R_d by light was partly a result of the artefact of changing Γ^*/C_c with irradiance. The real relative inhibition of R_d by light can be calculated as:

$$\text{Inhibition}_{\text{real}}(\%) = \frac{(R_{\text{D1measured}} - R_{\text{D2measured}}) - (R_{\text{D1modelled}} - R_{\text{D2modelled}})}{R_{\text{D1measured}}} \times 100 \quad \text{Eqn 5}$$

Compared with the relative apparent inhibition from the Yin method, the relative real inhibition was much lower (Fig. 6b). The results also suggested that after correcting for varying Γ^*/C_c, light inhibition of R_d only became lower but did not disappear: the real inhibition increased generally with relative amounts of photorespiration (Fig. 7).

Discussion

The 'linear decrease' of R_d with light cannot generate the Kok effect

The Kok effect was initially, and is still often, hypothesized to arise from the suppression of respiration by light (Fig. 1; Sharp *et al.*, 1984; Heskel *et al.*, 2013; Tcherkez *et al.*, 2017a; Way *et al.*, 2019). This hypothesis has received support from studies that have identified several mechanisms for the metabolic down-regulation of respiratory reactions by light, as reviewed by

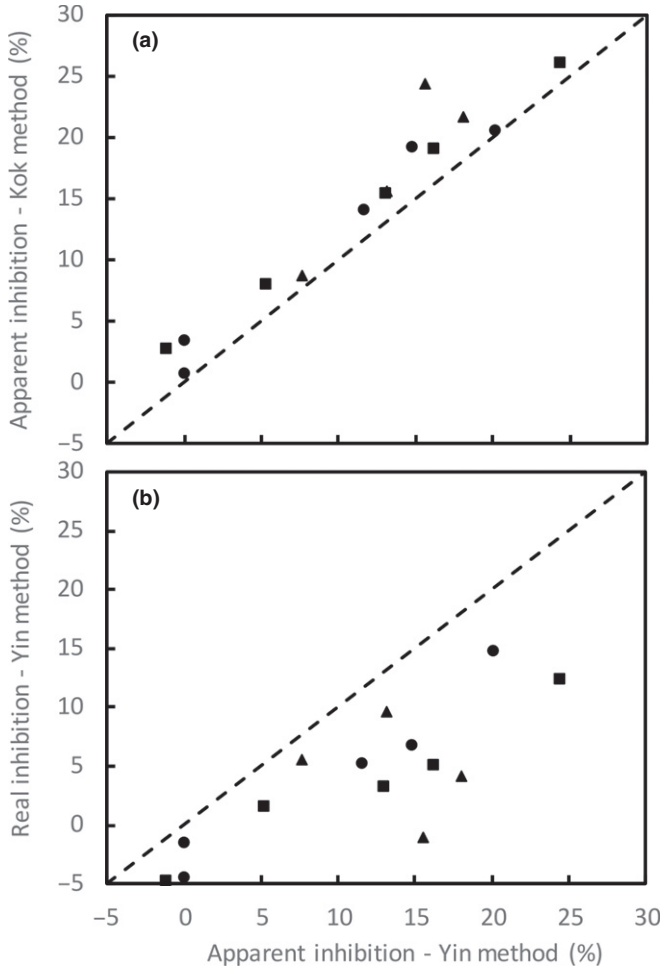

Fig. 6 Relative apparent light inhibition of day respiration, R_d, identified by the Kok method vs that identified by the Yin method (a), and relative real light inhibition vs the relative apparent light inhibition of R_d both identified by the Yin method (b), across various O_2 concentrations (circles), CO_2 concentrations (squares) and temperatures (triangles) for sunflower leaves. The dashed diagonal represents the 1 : 1 line, at which $y = x$.

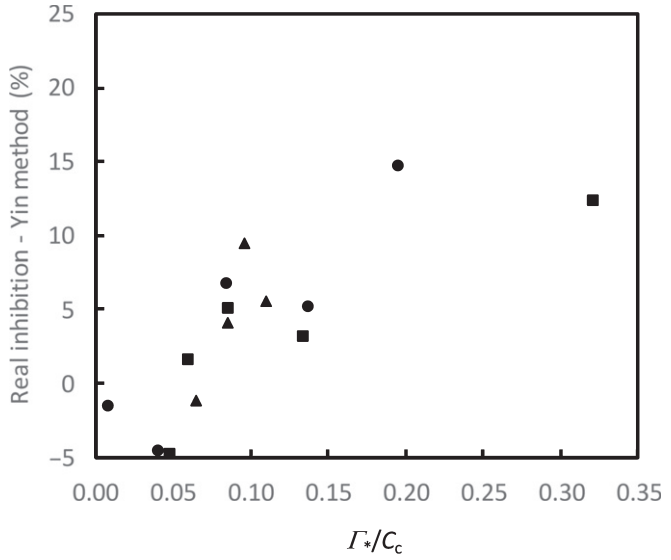

Fig. 7 The relative real light inhibition of respiration identified by the Yin method plotted against ratios of CO_2 compensation point to chloroplast CO_2 concentration (Γ^*/C_c) across various O_2 concentrations (circles), CO_2 concentrations (squares), and temperatures (triangles) for sunflower leaves.

Tcherkez *et al.* (2012, 2017b). Gas exchange measurements have shown that R_d, relative to R_{dk}, progressively decreased with increasing I_{abs}, either in a continuously linear manner (Villar *et al.*, 1994) or in a decelerating manner (Brooks & Farquhar, 1985; Villar *et al.*, 1995; Atkin *et al.*, 2000). Using Eqns 1–3, we assessed the effect of all possible scenarios for the often-said 'progressive' inhibition of respiration by light on the shape of $A-I_{abs}$ curves (Fig. 3). Of the six scenarios considered, only the three scenarios for 'decelerating decrease' of R_d with irradiance (Fig. 3b–d) can generate the Kok effect, thereby excluding the other three scenarios that are often considered relevant to the Kok effect. In particular, the scenario of a 'continuously linear decrease' of R_d with light (Fig. 3a) did not result in a break in the linear $A-I_{abs}$ relationship. This is in contrast to the statement of Tcherkez *et al.* (2017a) in their report for the 18th New Phytologist Workshop that 'the widely-accepted (historical) origin of the Kok effect is the inhibition of respiratory metabolism by light (linear decrease of R_d with light)'. Given the consequences of the various scenarios on the Kok effect, and thus also on the estimation of Φ_{CO2}, future studies should aim to reveal which of the three scenarios in Fig. 3 (b)–(d) is most likely for the light inhibition of R_d.

Several mechanisms co-contribute to the Kok effect

Our analyses suggest that not a single mechanism determines the Kok effect, but at least three mechanisms (i.e. decreasing Φ_2 with irradiance, varying Γ^*/C_c, and light inhibition of R_d) co-contribute to it. Using a model, we quantitatively estimated the relative contribution of the CO_2-specific processes like refixation (reflected via Γ^*/C_c) vs the light-dependent decrease in photochemical efficiency (Φ_2) in explaining the Kok effect. Our result suggested that varying Γ^*/C_c explained *c.* 25% of the Kok effect, while variable Φ_2 cannot be ignored and explained *c.* 12% of the Kok effect, across various CO_2, O_2 and temperature conditions. The appreciable contribution of variable Φ_2 is supported by decreases in the slope of phase 2, compared with Phase 1, of the $A-I_{abs}$ plots under conditions where photorespiration is greatly suppressed, for example, for C_3 species under low-O_2 conditions or for C_4 species (Yin *et al.*, 2011a).

However, there are still small decreases in the slope of phase 2 for C_3 species under low-O_2 conditions or for C_4 species when A was plotted against $I_{abs}\Phi_2$ (Yin *et al.*, 2011a). This effect in C_4 species may reflect the low efficacy of the CO_2-concentrating mechanism (CCM) caused by a high leakiness at low irradiances (Kromdijk *et al.*, 2010; Yin *et al.*, 2011b). However, for a C_3 species, Buckley *et al.* (2017) observed even more significant changes for developing leaves under 2% than under 21% O_2 conditions, suggesting an involvement of other mechanisms. A fourth mechanism was shown here to potentially contribute to the Kok effect (Fig. 2d), but we were not able to verify it, as any variable f_{aet} and/or ρ_2 are hard to identify at the light intensities showing the Kok effect. Our results, that $B_1 : B_2$ ratios (Table 2)

and R_{D1} : R_{D2} ratios (Table 3) were very close to 1 at 2% O_2 or 700 μmol mol^{-1} CO_2 suggest that significant involvement of a fourth mechanism was highly unlikely. Thus, our remaining unexplained part (*c.* 63%) of the Kok effect is most likely a result of the light suppression of R_d, in agreement with the statement of Buckley *et al.* (2017) on the dominant role of this third mechanism.

A dual effect of photorespiration in contributing to the Kok effect

Our strong linear relationships between the B_1 : B_2 ratio and the Γ^*/C_c ratio (Fig. 5a) confirmed previous results in the literature (Cornic & Jarvis, 1978; Ishii & Murata, 1972; Ishii & Schmid, 1981; Sharp *et al.*, 1984; Farquhar & Busch, 2017; Way *et al.*, 2019) showing that the Kok effect was strongly associated with the occurrence of photorespiration. Perhaps it is because of the significant contribution of varying Γ^*/C_c that the Kok effect reported in the earlier days (Kok, 1949; Ishii & Schmid, 1981; Sharp *et al.*, 1984) generally had sharper transition than the recent data (Farquhar & Busch, 2017; Tcherkez *et al.*, 2017a; Way *et al.*, 2019) because C_a has been increasing over years. However, the contribution of other factors as discussed earlier means that the Kok effect will never disappear in the future high-CO_2 atmosphere; instead, it will continue, but to a lesser extent.

Our modelling analysis suggests that strong associations between the B_1 : B_2 ratio and the Γ^*/C_c ratio shown in Fig. 5(a) are the combined result of a dual effect of photorespiration in contributing to the Kok effect. The first-type effect is what Farquhar & Busch (2017) discussed on the role of increasing Γ^*/C_c with irradiance in explaining the Kok effect, as a result of regulation of g_s and g_m. The second-type effect is what we found here – the light inhibition of R_d identified after removing the first-type effect was still positively correlated with Γ^*/C_c (Fig. 7). Our results suggest that the second-type effect, representing real biological inhibitions, probably contributed more to the Kok effect than the first-type effect.

Farquhar & Busch (2017) demonstrated that the first-type effect of photorespiration on the Kok effect can generate the apparent light inhibition of R_d for photorespiratory conditions. As stated in the introduction, this inhibition via regulation of g_s and g_m is the same as the importance that Loreto *et al.* (2001) emphasized for accounting for the refixation of respired CO_2 when estimating R_d. Loreto *et al.* (2001) stated that there would be no significant difference between R_d and R_{dk} if the refixation of respiratory CO_2 during illumination is taken into account. Our results showing that, after correcting for varying Γ^*/C_c, light inhibition of R_d only became lower but did not disappear (Fig. 6b), do not agree with the conclusion of Loreto *et al.* (2001). The refixation is an important means to reduce the (photo)respiratory loss under photorespiratory conditions, but its net contribution to total photosynthesis should be negligible under nonphotorespiratory conditions (Yin *et al.*, 2020). Berghuijs *et al.* (2019) showed that R_d estimated by the Kok method was closer to the estimate made by their model (that accounted for the refixation) under nonphotorespiratory than under photorespiratory conditions. The experiment of Loreto *et al.* (2001) was conducted with maize, a C_4 species where Rubisco is expected to be surrounded by a high CO_2 partial pressure as a result of the C_4 CCM, and thus the refixation of CO_2 released from respiration and photorespiration should have little contribution to the total assimilation. Using ^{14}C-labelling, Pärnik & Keerberg (1995, 2007a,b) showed that light inhibition of R_d occurs even when accounting for CO_2 refixation. Gong *et al.* (2015) reported a high suppression of R_d by light in a C_4 species. If refixation does occur appreciably in C_4 species as Loreto *et al.* stated, it may reflect the refixation more by phospho*enol*pyruvate carboxylase than by Rubisco, which might contribute to leakiness.

Apparent vs real light inhibition of R_d

The suppression of R_d by light has been identified using the Kok method, in many experimental studies, including recent reports based on CO_2-exchange measurements (e.g. Buckley *et al.*, 2017) or both CO_2- and O_2-exchange measurements (e.g. Gauthier *et al.*, 2018). Light is known to suppress the activity of enzymes that involve CO_2-releasing pathways contributing to R_d (Buckley & Adams, 2011; Tcherkez *et al.*, 2012, 2017a,b). Using the model analysis, Farquhar & Busch (2017) demonstrated that at least part of the light inhibition of R_d can be generated without assuming this inhibition beforehand. Here we used the modelling approach to analyse combined CO_2-exchange and Chl fluorescence data. With such combined experimental and modelling analyses, we demonstrated quantitatively that the original Kok method that attributes the Kok effect entirely to the light inhibition of R_d overestimated the real inhibition (Fig. 6), as a result of ignoring the contribution of varying Φ_2 and Γ^*/C_c to the Kok effect. The effect of varying Φ_2 on the Kok method in overestimating the inhibition has been corrected simply by the Yin method, while the correction for varying Γ^*/C_c is more complicated. We previously stressed that both Kok and Yin methods to estimate R_d actually apply to nonphotorespiratory conditions (Yin *et al.*, 2011a). Our analysis with Eqn 5 suggests an approach to estimate the real light suppression of R_d for photorespiratory conditions, although we are unable to clarify which one of the three scenarios of suppression in Fig. 3(b–d) is most likely. Most importantly, our analysis using Eqn 5 revealed that the real suppression still increased with relative amounts of photorespiration (Fig. 7). While this new empirical trend receives the support from a theoretical analysis of Buckley & Adams (2011) that photorespiratory NADH may be involved in the suppression, there are probably other underlying biochemical mechanisms that merit further investigation.

Author contributions

XY conceived the study, XY and PELvdP designed the experiment, YN and PELvdP implemented the experiment and conducted the measurements, XY and YN analysed the data, and XY wrote the draft and finalised it with significant input from PCS.

ORCID

Paul C. Struik https://orcid.org/0000-0003-2196-547X
Xinyou Yin https://orcid.org/0000-0001-8273-8022

References

Amthor JS. 2010. From sunlight to phytomass: on the potential efficiency of converting solar radiation to phyto-energy. *New Phytologist* **188**: 939–959.

Atkin OK, Evans JR, Ball MC, Lambers H, Pons TL. 2000. Leaf respiration of snow gum in the light and dark. Interactions between temperature and irradiance. *Plant Physiology* **122**: 915–923.

Ayub G, Smith RA, Tissue DT, Atkin OK. 2011. Impacts of drought on leaf respiration in darkness and light in *Eucalyptus saligna* exposed to industrial-age atmospheric CO_2 and growth temperature. *New Phytologist* **190**: 1003–1018.

Berghuijs HNC, Yin X, Ho QT, Retta MA, Nicolaï BM, Struik PC. 2019. Using a reaction-diffusion model to estimate day respiration and reassimilation of (photo)respired CO_2 in leaves. *New Phytologist* **223**: 619–631.

Bernacchi CJ, Portis AR, Nakano H, von Caemmerer S, Long SP. 2002. Temperature response of mesophyll conductance. Implication for the determination of Rubisco enzyme kinetics and for limitations to photosynthesis *in vivo*. *Plant Physiology* **130**: 1992–1998.

Brooks A, Farquhar GD. 1985. Effect of temperature on the CO_2/O_2 specificity of ribulose-1,5-bisphosphate carboxylase/oxygenase and the rate of respiration in the light. *Planta* **165**: 397–406.

Buckley TN, Adams MA. 2011. An analytical model of non-photorespiratory CO_2 release in the light and dark in leaves of C_3 species based on stoichiometric flux balance. *Plant, Cell & Environment* **34**: 89–112.

Buckley TN, Vice H, Adams MA. 2017. The Kok effect in *Vicia faba* cannot be explained solely by changes in chloroplastic CO_2 concentration. *New Phytologist* **216**: 1064–1071.

Cornic G, Jarvis PG. 1972. Effects of oxygen on CO_2 exchange and stomatal resistance in Sitka spruce and maize at low irradiances. *Photosynthetica* **6**: 225–239.

Evans JR, von Caemmerer S. 1996. Carbon dioxide diffusion inside leaves. *Plant Physiology* **110**: 339–346.

Farquhar GD, Busch FA. 2017. Changes in the chloroplastic CO_2 concentration explain much of the observed Kok effect: a model. *New Phytologist* **214**: 570–584.

Farquhar GD, von Caemmerer S, Berry JA. 1980. A biochemical model of photosynthetic CO_2 assimilation in leaves of C_3 species. *Planta* **149**: 78–90.

Gauthier PPG, Battle MO, Griffin KL, Bender ML. 2018. Measurement of gross photosynthesis, respiration in the light, and mesophyll conductance using $H_2{}^{18}O$ labelling. *Plant Physiology* **177**: 62–74.

Genty B, Harbinson J. 1996. Regulation of light utilization for photosynthetic electron transport. In: Baker NR, ed. *Photosynthesis and the Environment. Vol 5 book series 'Advances in Photosynthesis and Respiration'*. The Netherlands: Kluwer Academic Publishers, 67–99.

Gifford RM. 1995. Whole plant respiration and photosynthesis of wheat under increased CO_2 concentration and temperature: long-term vs. short-term distinctions from modelling. *Global Change Biology* **1**: 385–396.

Gong XY, Schäufele R, Feneis W, Schnyder H. 2015. $^{13}CO_2/^{12}CO_2$ exchange fluxes in a clamp-on leaf cuvette: disentangling artefacts and flux components. *Plant, Cell & Environment* **38**: 2417–2432.

Gong XY, Schäufele R, Lehmeier CA, Tcherkez G, Schnyder H. 2017. Atmospheric CO_2 mole fraction affects stand-scale carbon use efficiency of sunflower by stimulating respiration in light. *Plant, Cell & Environment* **40**: 401–412.

Gong XY, Tcherkez G, Wenig J, Schäufele R, Schnyder H. 2018. Determination of leaf respiration in the light: comparison between an isotopic disequilibrium method and the Laisk method. *New Phytologist* **218**: 1371–1382.

Harley PC, Loreto F, Di Marco G, Sharkey TD. 1992. Theoretical considerations when estimating the mesophyll conductance to CO_2 flux by analysis of the response of photosynthesis to CO_2. *Plant Physiology* **98**: 1429–1436.

Healey FP, Myers J. 1971. The Kok effect in *Chlamydomonas reinhardi*. *Plant Physiology* **47**: 373–379.

Heskel MA, Atkin OK, Turnbull MH, Griffin KL. 2013. Bringing the Kok effect to light: A review on the integration of daytime respiration and net ecosystem exchange. *Ecosphere* **4**: 1–14.

Ishii R, Murata Y. 1978. Further evidence of the Kok effect in C_3 plants and the effects of environmental factors on it. *Japanese Journal of Crop Science* **47**: 547–550.

Ishii R, Schmid GH. 1981. The Kok effect and its relationship to photorespiration in tomato. *Zeitschrift für Naturforschung* **36c**: 450–454.

Kirschbaum MUF, Farquhar GD. 1987. Investigation of the CO_2 dependence of quantum yield and respiration in *Eucalyptus pauciflora*. *Plant Physiology* **83**: 1032–1036.

Kok B. 1948. A critical consideration of the quantum yield of *Chlorella*-photosynthesis. *Enzymologia* **13**: 1–56.

Kok B. 1949. On the interrelation of respiration and photosynthesis in green plants. *Biochemica et Biophysica Acta* **3**: 625–631.

Kromdijk J, Griffiths H, Schepers HE. 2010. Can the progressive increase of C_4 bundle sheath leakiness at low PFD be explained by incomplete suppression of photorespiration? *Plant, Cell & Environment* **33**: 1935–1948.

Laisk AK. 1977. *Kinetics of photosynthesis and photorespiration in C_3 plant.* Moscow, Russia: Nauka (in Russian).

Long SP, Postl WF, Bolhár-Nordenkampf HR. 1993. Quantum yields for uptake of carbon dioxide in C_3 vascular plants of contrasting habitats and taxonomic groupings. *Planta* **189**: 226–234.

Loreto F, Velikova V, Di Marco G. 2001. Respiration in the light measured by $^{12}CO_2$ emission in $^{13}CO_2$ atmosphere in maize leaves. *Australian Journal of Plant Physiology* **28**: 1103–1108.

Pärnik T, Keerberg O. 1995. Decarboxylation of primary and end products of photosynthesis at different oxygen concentrations. *Journal of Experimental Botany* **46**: 1439–1477.

Pärnik T, Keerberg O. 2007a. Advanced radiogasometric method for the determination of the rates of photorespiratory and respiratory decarboxylations of primary and stored photosynthates under steady-state photosynthesis. *Physiologia Plantrum* **129**: 33–44.

Pärnik T, Keerberg O. 2007b. Photorespiratory and respiratory decarboxylations in leaves of C_3 plants under different CO_2 concentrations and irradiances. *Plant, Cell & Environment* **30**: 1535–1544.

Peltier G, Sarrey F. 1988. The Kok effect and the light-inhibition of chlororespiration in *Chlamydomonas reinhardtii*. *FEBS Letters* **228**: 259–262.

Pinelli P, Loreto F. 2003. $^{12}CO_2$ emission from different metabolic pathways measured in illustrated and darkened C_3 and C_4 leaves at low, atmospheric and elevated CO_2 concentration. *Journal of Experimental Botany* **54**: 1761–1769.

Sharp RE, Matthews MA, Boyer JS. 1984. Kok effect and the quantum yield of photosynthesis. Light partially inhibits dark respiration. *Plant Physiology* **75**: 95–101.

Tcherkez G, Boex-Fontvieille E, Mahe A, Hodges M. 2012. Respiratory carbon fluxes in leaves. *Current Opinion in Plant Biology* **15**: 308–314.

Tcherkez G, Gauthier P, Buckley TN, Busch FA, Barbour MM, Heskel DA, Gong XY, Crous K, Griffin KL, Way DA *et al.* 2017a. Tracking the origins of the Kok effect, 70 years after its discovery. *New Phytologist* **214**: 506–510.

Tcherkez G, Gauthier P, Buckley TN, Busch FA, Barbour MM, Heskel DA, Gong XY, Crous KY, Griffin K, Way D *et al.* 2017b. Leaf day respiration: low CO_2 flux but high significance for metabolism and carbon balance. *New Phytologist* **216**: 986–1001.

Tholen D, Ethier G, Genty B, Pepin S, Zhu X-G. 2012. Variable mesophyll conductance revisited: theoretical background and experimental implications. *Plant, Cell & Environment* **35**: 2087–2103.

Ubierna N, Cernusak LA, Holloway-Phillips M, Busch FA, Cousins AB, Farquhar GD. 2019. Critical review: incorporating the arrangement of mitochondria and chloroplasts into models of photosynthesis and carbon isotope discrimination. *Photosynthesis Research* **141**: 5–31.

Ver Sagun J, Badger MR, Chow WS, Ghannoum O. 2019. Cyclic electron flow and light partitioning between the two photosystems in leaves of plants with different functional types. *Photosynthesis Research* **142**: 321–334.

Villar R, Held AA, Merino J. 1994. Comparison of methods to estimate dark respiration in the light of leaves of two woody species. *Plant Physiology* **105**: 167–172.

Villar R, Held AA, Merino J. 1995. Dark leaf respiration in light and darkness of an evergreen and a deciduous plant species. *Plant Physiology* **107**: 421–427.

von Caemmerer S. 2013. Steady-state models of photosynthesis. *Plant, Cell & Environment* **36**: 1617–1630.

von Caemmerer S, Evans JR. 2015. Temperature responses of mesophyll conductance differ greatly between species. *Plant, Cell & Environment* **38**: 629–637.

Walker BJ, Ariza LS, Kaines S, Badger MR, Cousins AB. 2013. Temperature response of *in vivo* Rubisco kinetics and mesophyll conductance in *Arabidopsis thaliana*: comparisons to *Nicotiana tabacum*. *Plant, Cell & Environment* **36**: 2108–2119.

Warren CR, Dreyer E. 2006. Temperature response of photosynthesis and internal conductance to CO_2: results from two independent approaches. *Journal of Experimental Botany* **57**: 3057–3067.

Way DA, Aspinwall MJ, Drake JE, Crous KY, Campany CE, Ghannoum O, Tissue DT, Tjoeker MG. 2019. Responses of respiration in the light to warming in field-grown trees: a comparison of the thermal sensitivity of the Kok and Laisk methods. *New Phytologist* **222**: 132–143.

Yin X, Belay DW, van der Putten PEL, Struik PC. 2014. Accounting for the decrease of photosystem photochemical efficiency with increasing irradiance to estimate quantum yield of leaf photosynthesis. *Photosynthesis Research* **122**: 323–335.

Yin X, Harbinson J, Struik PC. 2006. Mathematical review of literature to assess alternative electron transports and interphotosystem excitation partitioning of steady-state C_3 photosynthesis under limiting light. *Plant, Cell & Environment* **29**: 1771–1782. (Corrig. in *Plant, Cell & Environment* **29**: 2252).

Yin X, Struik PC. 2009. Theoretical reconsiderations when estimating the mesophyll conductance to CO_2 diffusion in leaves of C_3 plants by analysis of combined gas exchange and chlorophyll fluorescence measurements. *Plant, Cell & Environment* **32**: 1513–1524. (Corrig. in *Plant, Cell & Environment* **33**: 1595).

Yin X, Struik PC. 2017. Simple generalisation of a mesophyll resistance model for various intracellular arrangements of chloroplasts and mitochondria in C_3 leaves. *Photosynthesis Research* **132**: 211–220.

Yin X, Struik PC, Romero P, Harbinson J, Evers JB, van der Putten PEL, Vos J. 2009. Using combined measurements of gas exchange and chlorophyll fluorescence to estimate parameters of a biochemical C_3 photosynthesis model: a critical appraisal and a new integrated approach applied to leaves in a wheat (*Triticum aestivum*) canopy. *Plant, Cell & Environment* **32**: 448–464.

Yin X, Sun Z, Struik PC, Gu J. 2011a. Evaluating a new method to estimate the rate of leaf respiration in the light by analysis of combined gas exchange and chlorophyll fluorescence measurements. *Journal of Experimental Botany* **62**: 3489–3499.

Yin X, Sun Z, Struik PC, van der Putten PEL, van Ieperen W, Harbinson J. 2011b. Using a biochemical C_4-photosynthesis model and combined gas exchange and chlorophyll fluorescence measurements to estimate bundle-sheath conductance of maize leaves differing in age and nitrogen content. *Plant, Cell & Environment* **34**: 2183–2199.

Yin X, van der Putten PEL, Belay D, Struik PC. 2020. Using photorespiratory oxygen response to analyse leaf mesophyll resistance. *Photosynthesis Research* **144**: 85–99.

Yin X, van Oijen M, Schapendonk AHCM. 2004. Extension of a biochemical model for the generalized stoichiometry of electron transport limited C_3 photosynthesis. *Plant, Cell & Environment* **27**: 1211–1222.

Zhang M-M, Fan D-Y, Sun GY, Chow WS. 2018. Optimising the linear electron transport rate measured by chlorophyll *a* fluorescence to empirically match the gross rate of oxygen evolution in white light: towards improved estimation of the cyclic electron flux around photosystem I in leaves. *Functional Plant Biology* **45**: 1138–1148.

Supporting Information

Additional Supporting Information may be found online in the Supporting Information section at the end of the article.

Fig. S1 Photosystem II photochemical efficiency (Φ_2) as a function of absorbed irradiance (I_{abs}) across various O_2 and CO_2 concentrations and various temperatures.

Fig. S2 Comparison of net photosynthesis rate A and the average Γ^*/C_c ratio modelled using three mesophyll conductance g_m modes as described in the text.

Table S1 List of all model symbols.

Table S2 Model parameter values estimated using three mesophyll conductance g_m modes.

Please note: Wiley Blackwell are not responsible for the content or functionality of any Supporting Information supplied by the authors. Any queries (other than missing material) should be directed to the *New Phytologist* Central Office.